Physics and Imaging in Radiation Oncology 9 (2019) 77–82

Contents lists available at ScienceDirect

Physics and Imaging in Radiation Oncology

journal homepage: www.elsevier.com/locate/phro

Original Research Article

Cervical cancer apparent diffusion coefficient values during external beam radiotherapy

Peter de Boer[a,b,*], Stefano Mandija[c], Anita M. Werensteijn-Honingh[a], Cornelis A.T. van den Berg[c], Astrid A.C. de Leeuw[a], Ina M. Jürgenliemk-Schulz[a]

[a] Department of Radiation Oncology, University Medical Centre Utrecht, The Netherlands
[b] Department of Radiation Oncology, Amsterdam University Medical Centres (Amsterdam UMC) – University of Amsterdam (UvA), The Netherlands
[c] Centre for Image Sciences, University Medical Centre Utrecht, Heidelberglaan 100, Utrecht 3584 CX, The Netherlands

ARTICLE INFO

Keywords:
Cervical cancer
ADC map
MRI

ABSTRACT

Background and purpose: Apparent diffusion coefficient (ADC) reflects micro-enviromental changes and therefore might be useful in predicting recurrence prior to brachytherapy. The purpose of this study is to evaluate change in ADC of the primary tumour and pathologic lymph nodes during treatment and to correlate this with clinical outcome.

Material and methods: Twenty patients were included who received chemoradiation for locally advanced cervical cancer between July 2016 and November 2017. All patients underwent magnetic resonance imaging (MRI) prior to treatment, and three MRIs in weeks 1/2, 3 and 4 of treatment, including T2 and diffusion weighted imaging (*b*-values 0, 200, 800 s/mm^2) for determining an ADC-map. Primary tumour was delineated on T2 and ADC-map and pathologic lymph nodes were delineated only on ADC-map.

Results: At time of analysis median follow-up was 15 (range 7–22) months. From MRI one to four, primary tumour on ADC-map showed a significant signal increase of 0.94 (range 0.74–1.46) $\times 10^{-3}$ mm^2/s to 1.13 (0.98–1.49) $\times 10^{-3}$ mm^2/s ($p < 0.001$). When tumour was delineated on T2, ADC-value signal increase (in tumour according to T2) was similar. All 46 delineated pathologic lymph nodes showed an ADC-value increase on average from 0.79 (range 0.33–1.12) $\times 10^{-3}$ mm^2/s to 1.14 (0.59–1.75) $\times 10^{-3}$ mm^2/s ($p < 0.001$). The mean tumour/suspected lymph node volumes decreased respectively 51/40%. Four patients developed relapse (one local and three nodal), without clear relation with ΔADC. However, the median volume decrease of the primary tumour was substantially lower in the failing patients compared to the group without relapse (19 vs. 57%).

Conclusions: ADC values can be acquired using T2-based tumour delineations unless there are substantial shifts between ADC-mapping and T2 acquisition. It remains plausible that ΔADC is a predictor for response to EBRT. However, the correlation in this study was not statistically significant.

1. Introduction

Cervical cancer is a major global problem as it is the fourth most common cancer in women, with an incidence of 528,000 women/year and causing 266,000 deaths in 2012 [1]. About 40% of the patients are diagnosed with locally advanced disease (LACC), for whom chemoradiation (CRT) is considered the standard curative care [2–4]. During the last decades, MRI-guided adaptive brachytherapy has resulted in an approximately 20% improvement in 5-year local control (LC) [5–10]. However, opportunities remain for further improving LC, especially for patients with primary tumours > 30 cm^3 at the time of brachytherapy and for FIGO stage IIIA–IVA, as reported LC for the latter group is only 71–79% after 5 years [5,11]. Data published by the EMBRACE-group revealed the crucial importance of 90% tumour coverage with an adequate brachytherapy dose (≥85 Gy) for achieving LC [12,13]. A further step in LC might be achieved by determining which tumours are at risk of local recurrence and might benefit from further dose escalation at the time of brachytherapy.

In western countries, T2-weighted MRI with its superior soft tissue contrast compared to CT, is widely used for evaluating tumour spread in the staging of cervical cancer [14,15]. For tissue characterisation, such as differentiation between residual tumour and radiation-induced

* Corresponding author at: Dept. of Radiation Oncology, Amsterdam UMC, UvA, Meibergdreef 9, 1105 AZ Amsterdam, The Netherlands.
E-mail address: p.deboer@amc.uva.nl (P. de Boer).

https://doi.org/10.1016/j.phro.2019.03.001
Received 7 September 2018; Received in revised form 28 February 2019; Accepted 1 March 2019

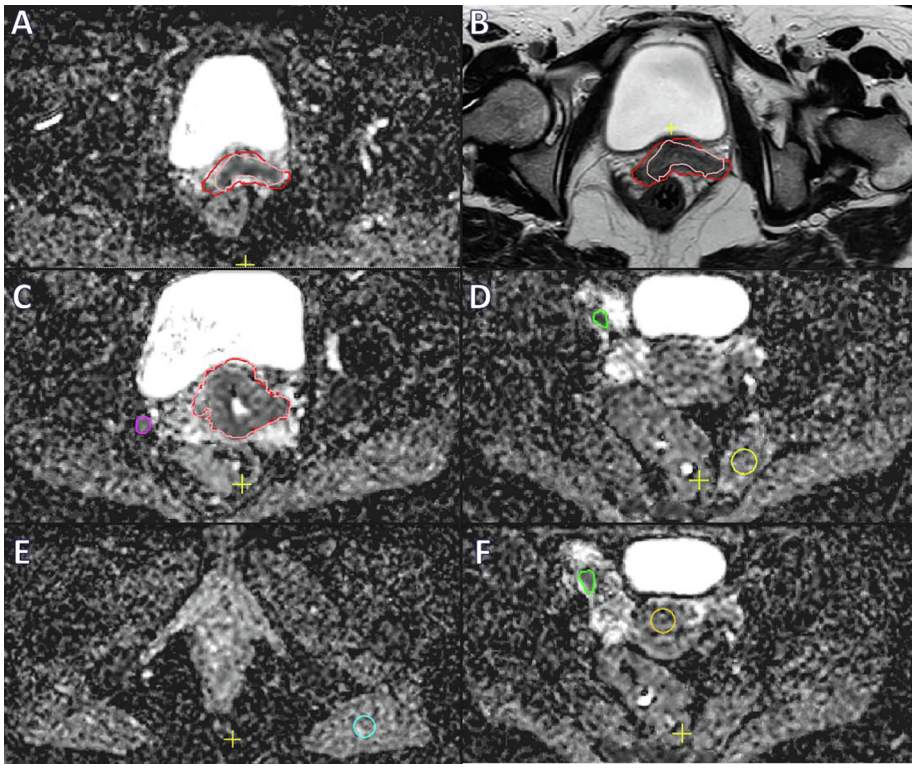

Fig. 1. Delineation of a 53-year old women with FIGO stage IIB cervical cancer. Delineation of the primary tumour on ADC-map in pink is visualised in A, while in B the tumour is delineated on T2 weighted imaging (red). In C delineation of a pathological lymph node on ADC-map is shown (purple), and in F (green). Additionally three reference volumes (S1–3) were created in smooth muscle: S1 within the high dose EBRT (45 Gy) area (image D, yellow), S2 well below the caudal border of the planned radiotherapy field (image E, blue), and S3 (image F, orange) within the uninvaded part of the uterine corpus. (For interpretation of the references to colour in this figure legend, the reader is referred to the web version of this article.)

changes, other sequences might be needed. Diffusion weighted MR imaging (DWI) visualises restriction in water mobility in tissue. Micro-environmental pathologic conditions such as the content of malignant tumour tissue change the water mobility and could be used as an early biomarker of response to CRT [16]. DWI is susceptible to T2 shine through effect for low *b*-values and to low signal to noise ratio (SNR) for relatively high *b*-values [17]. These effects can be mitigated and optimal tissue characterisation can be achieved by quantifying the water mobility on a voxel basis by the so-called apparent diffusion coefficient (ADC) [17]. This parameter can be determined by fitting an exponential decay to the signal in various images with various *b*-values.

With ADC-mapping, one can differentiate between malignant and non-malignant tissue in a region of interest with good test characteristics (sensitivity 96%, specificity 100%) [18]. Furthermore, alteration of mean ADC values (ΔADC) is higher in complete responders compared to partial and non-responders, and therefore could predict local recurrence prior to brachytherapy [19–23].

Since ADC mappings can chart micro-environmental changes in target areas, it might be used to reduce delineation uncertainties and to better differentiate between complete and partial/non-responders at the time of brachytherapy. Brachytherapy treatment could be adapted accordingly, by escalating the dose for partial/non-responders. In this study we have investigated the correlation of the ΔADC of the primary tumour during treatment to clinical outcome (disease recurrence), based on weekly MRI during external beam radiotherapy (EBRT), also taking into account FIGO stage and tumour volume. Furthermore, we have investigated mean ΔADC in pathologic lymph nodes and its correlation with primary tumour ΔADC.

2. Materials and methods

2.1. Patients & treatment

After approval of the institutional ethics review board, twenty patients with cervical cancer that were eligible for definitive CRT (FIGO stage IB2-IVA and patients with pathological lymph nodes) were included in a mono-centre imaging study (CeReMony). All patients received chemoradiation which consisted of EBRT 45 Gy in 25 daily fractions, with simultaneous integrated boost (SIB) for pathological lymph nodes to 57.5 Gy for para-aortic and common iliac nodes, and to 55 Gy for pathological lymph nodes within the pelvis. All fractions were delivered with a volumetric arc therapy (VMAT) technique. MRI-guided adaptive brachytherapy was given after two implantations in a total of four fractions (2 × 2) with high dose rate aiming at a CTV_{HR} $D_{90\%}$ > 90 Gy $EQD2_{10}$ according to the EMBRACE II protocol [9,10,13]. Patients underwent implantation with tandem and ovoid applicators compatible with the intracavitary-interstitial technique.

2.2. Imaging protocol

As part of the CeReMony study, all patients underwent three MRIs during EBRT treatment. The MRI protocol included three T2 weighted, multislice, turbo spin echo (TSE) sequences. For sagittal, coronal and transversal orientations, the repetition time/echo time (TR/TE) were respectively 4518/100 ms, 4649/100 ms, and 6332/100 ms; the TSE echo spacing/shot length 5.6/194 ms, 7.7/192 ms, and 7.7/192 ms. For these three MRI sequences the image resolution was $0.9 \times 0.9 \times 3\,mm^3$, and the reconstructed voxel size was $0.5 \times 0.5 \times 3\,mm^3$. Additionally, a DWI with fat suppression (Spectral Attenuated Inversion Recovery, SPAIR) was acquired using a single shot EPI readout (EPI factor: 53; TR/TE = 12073/75 ms; voxel size 2.5 × 2.5 × 4.0 mm). From this sequence, the apparent diffusion coefficient (ADC) map was determined by voxel-based, mono-exponential fitting of the three diffusion weighted images acquired with the following *b*-values: 0, 200 and 800 s/mm^2 with respectively 2, 2, and 4 signal averages (NSA).

Thereby, the following equation was used: $S(b) = S(0)^{-b\,ADC}$

All MRI acquisitions were made on the same Philips 1,5 Tesla MRI scanner (MR-RT Ingenia, Philips Medical Systems, Best, The Netherlands) in supine treatment position using anterior (dStream Torso array) and integrated posterior coil arrays. A total of 4 MRI's were made (MRI 1–4); the first MRI was performed before starting

EBRT, the consecutive MRI's were planned during treatment in week 1, 3 and 4 or in week 2, 3 and 4 of the EBRT treatment. The last MRI was made before brachytherapy implantation in week 4 of EBRT treatment. During follow-up routine T2 weighted MR images (without ADC mapping) were made at 3 and 12 months after treatment, or when there was clinical suspicion for recurrence.

2.3. Target definition and delineation

On all MRI's visible tumour (GTV) was separately delineated on T2 sequence (GTV_{T2}), and on the ADC-map (GTV_{ADC}) by one experienced radiation oncology resident (Fig. 1). GTV_{T2} is generally well visible on T2-weighted imaging and was delineated according to existing recommendations [9,10]. Typically for GTV_{ADC}, the tumour showed a lower signal on ADC-map which was more homogenous than the surrounding tissue. Delineations were thoroughly checked and, if needed, adjusted after reaching consensus by a radiation oncologist with 20 years of experience within the field of gynaecological oncology. Furthermore, all lymph nodes that were considered metastatic (based on diagnostic MRI and PET-CT) by the multidisciplinary tumour board were delineated on the ADC map (GTV_{Nx}). Additionally three reference volumes (S1–3) were created in smooth muscle: one within the high dose EBRT (45 Gy) area (S1), one well below the caudal border of the planned radiotherapy field (S2), and one within the uninvaded part of the uterine corpus (S3).

2.4. Analysis

After confirming normality by using the Shapiro-Wilk test, a two-sided paired *t*-test was used to compare the volumes of GTV_{T2} and GTV_{ADC}. In order to investigate the ADC value in visible tumour and its concordance with the ADC value of suspected lymph nodes during treatment, mean ADC-values and standard deviations (SD) of GTV_{ADC}, GTV_{Nx}, and reference volumes were calculated and visualised. If no normality was confirmed by neither visual evaluation of histograms nor the Shapiro-Wilk test, the Friedmans test was used for analyses. Thereby comparing the concordance of each lymph node with the primary tumour of that particular patient. The significance of difference in ADC values during treatment (ΔADC) was evaluated using Friedmans test. Concordance between GTV_{ADC} and GTV_{Nx} was calculated using the Wilcoxon signed rank test.

3. Results

Twenty patients were included with a median follow-up of 15 months (range 7–22 months) at time of analysis (May 2018). Baseline characteristics are summarised in Table 1. Median age at time of treatment was 50 years (range 29–70 years). All patients received the first MRI one to three weeks before treatment. Afterwards, five patients had MRI 2–4 in week 1, 3 and 4, and 15 patients in week 2, 3 and 4 during EBRT treatment. One patient did not endure the MR acquisition during week 2, and one did not during week 3. These data were excluded from the analysis. A total of 46 lymph nodes suspicious for nodal metastases were identified in 13 patients (median per patient 2, range 1–10). Two patients showed complete local radiological response on MRI in week 4 and one of these patients already in week 3.

Before treatment the mean volumes were GTV_{ADC} 50 cm^3 (range 19–125 cm^3, SD 33 cm^3), GTV_{T2} 51 cm^3 (range 19–125 cm^3, SD 32 cm^3) and GTV_{Nx} 1.1 cm^3 (range 0.1–4.0 cm^3, SD 1.1 cm^3). A paired sample *t*-test revealed that the volume reductions of GTV_{T2} in week 4 of treatment, as compared to MRI 1 (mean 54%, SD 26%, range 7–100%), were not significantly different from GTV_{ADC} volume reductions (mean 51%, SD 29% range 2–100%) as ($p = 0.31$). Mean pathologic lymph node volume reduction during the course of treatment was 40% (SD 48%, range −113% to 90%, $p < 0.001$). In 7/46 of the pathologic lymph nodes there was an overall increase in lymph node volume during treatment.

Table 1
Baseline characteristics. FIGO = International Federation of Gynaecology and Obstetrics; SCC = squamous cell carcinoma; AC = adenocarcinoma; ASC = adenosqaumous carcinoma.

Parameter	Value
Number of patients (n)	20
Median age at start of radiotherapy treatment (years)	50(29–70)
Median follow up (months)	15 (7–22)
FIGO stage	
IB	4
IIA	1
IIB	9
IIIB	6
Histopathological subtype	
SCC	15
AC	4
ASC	1
Nodal disease	
Number of patients	13
Median number of nodes/patient	2 (0–10)
Timing of MRI 1–4 (n)	
Week 0-2-3-4	15
Week 0-1-3-4	5

Compared to the pre-treatment situation, GTV_{ADC} ADC values showed a significant average increase from MRI 1 to 4 starting from 0.94 (range 0.74–1.46) $\times 10^{-3}$ mm^2/s at MRI 1, 1.04 (0.79–1.59) $\times 10^{-3}$ mm^2/s at MRI 2, 1.12 (0.84–1.57) $\times 10^{-3}$ mm^2/s at MRI 3 up to 1.13 (0.98–1.49) $\times 10^{-3}$ mm^2/s ($p < 0.001$) at MRI 4 (Fig. 2). ADC values of GTV_{T2} show a similar increase at MRI1–4 from 0.96 (range 0.72–1.46) $\times 10^{-3}$ mm^2/s, 1.00 (0.62–1.65) $\times 10^{-3}$ mm^2/s, 1.10 (0.87–1.59) $\times 10^{-3}$ mm^2/s, up to 1.10 (0.7–1.59) $\times 10^{-3}$ mm^2/s ($p < 0.001$), respectively. GTV_{ADC} GTV_{T2} and GTV_{Nx} ADC values dit not resemble a normal distribution when plotted in a histogram (not shown), this was confirmed by the Shapiro-Wilk test which tested below 0.84 in MRI1–4. ADC values from GTV_{T2} were not significantly different compared to ADC value in GTV_{ADC}, although on T2 there was a slightly higher standard deviation (0.43 vs. 0.37 $\times 10^{-3}$ mm^2/s). From MRI1 to MRI4, ADC values within GTV_{Nx} showed an average increase from 0.79 (range 0.33–1.12) $\times 10^{-3}$ mm^2/s at MRI 1, 0.89 (0.54–1.39) $\times 10^{-3}$ mm^2/s at MRI 2, 1.02 (0.56–1.44) $\times 10^{-3}$ mm^2/s at MRI 3 up to 1.14(0.59–1.75) $\times 10^{-3}$ mm^2/s ($p < 0.001$) at MRI 4 (Fig. 3). There was no paired correlation found between ADC value increase of GTV_{ADC}

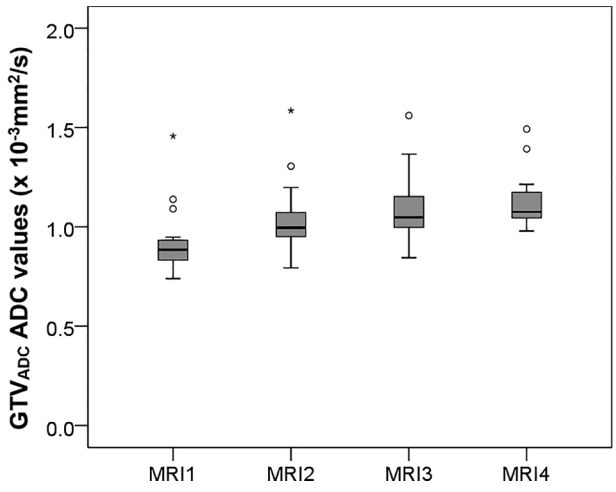

Fig. 2. GTV_{ADC} ADC values at baseline (MRI 1) and during treatment (MRI2–4) shows significant increase in ADC values ($p < 0.001$).

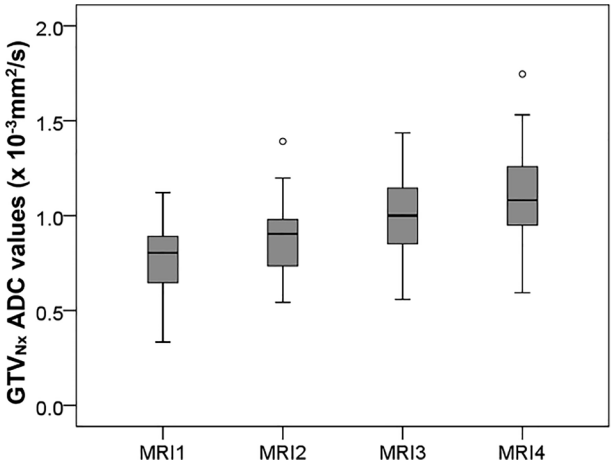

Fig. 3. GTV_{Nx} ADC values of suspected lymph nodes at baseline (MRI 1) and during treatment (MRI2–4).

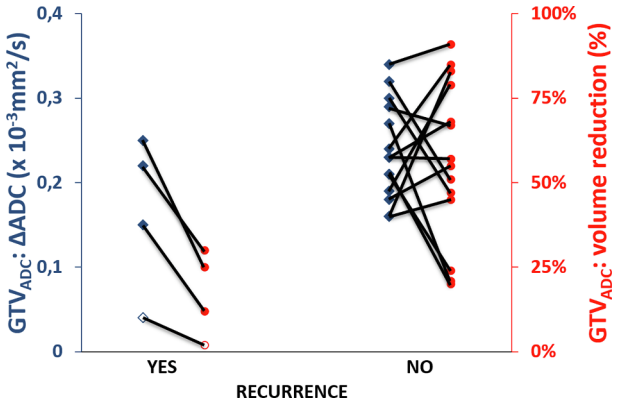

Fig. 4. Overall relapse in relation to ADC value increase (blue diamonds) and volume reduction (red circles) in GTV_{ADC}. Each case is connected by a line to visualise relation between outcomes of individual patients. Red: eighty percent of the patients with no recurrence after 12 months show a GTV_{ADC} reduction of > 47%, while patients with a recurrence have a tumour reduction of no more than 30% in this study. Blue: ADC increase of patients with a recurrence is only slightly lower than patients that have no sign of recurrence. The 'hollow' data points indicate a local relapse whereas the other three patients recurred regionally of whom 2 also distantly. (For interpretation of the references to colour in this figure legend, the reader is referred to the web version of this article.)

and GTV_{Nx} within the same patients. The ADC values in reference sample volumes S1, S2, and S3 did not significantly increase or decrease during treatment.

After 3 months 12/20 and 12 months 19/20 of the patients showed complete radiological response to treatment. Four patients developed a relapse according to radiology reports (Table 2). Patient 1 had regional and distant relapse 6 months after treatment. When comparing with MRI before treatment, three lymph node recurrences could be identified within the initially boost target volumes and had received ≥57.5 Gy. Seven lymph node recurrences were in the electively treated volume but without visible nodes in the respective region at time of diagnosis. Three of them were near high dose boost volumes and got approximately 55 Gy or more, and 4 got elective dose only. The three nodes which were identified as target volumes at initial treatment planning could be identified on ADC mapping on MRI 1–4 and showed ΔADC during treatment of $0.08 \times 10^{-3}\,mm^2/s$, $0.57 \times 10^{-3}\,mm^2/s$ and $0.42 \times 10^{-3}\,mm^2/s$. Patient 2 showed at 9 months diffuse regional and distant relapse with one node that was within a boost target volume. This lymph node showed a ΔADC between MRI 1 and 4 of $0.75 \times 10^{-3}\,mm^2/s$. Patient 3 showed a relapse in the primary tumour region on routine MRI at 12 months which was confirmed by histopathology. Patient 4 had relapse also at 12 months after treatment in an obturator lymph node close to the right parametrium. As shown in Fig. 4, all four patients with a recurrence showed a maximum GTV_{ADC} volume reduction during treatment of 30%, while 13/16 (81%) of the patients without recurrence had GTV_{ADC} volume reduction well above this 30%. Similar results were found when GTV was delineated on T2 (not shown). The maximum volume reductions of GTV_{T2} in patients with a recurrence was 37%, and 13/16 (81%) of the patients without recurrence showed a volume reduction of > 41%. A relation between ΔADC values and recurrence was not found.

There were no significant correlations between $GTV_{ADC/T2/Nx}$ volume reductions/ΔADC and/or baseline characteristics. The correlation found between volume reduction and ADC increase of the GTV_{ADC} volume was small and not significant (Pearson correlation coefficient 0.43, p = 0.07) as visualised in Fig. 5. No relation between lymph node volume change, lymph node ΔADC and recurrence was found (Fig. A.1). If ADC values per patients were plotted, four patients have overall higher ADC values in GTV_{ADC} than the rest of the patients (see Fig. A.2). In the ADC plot of all separate 46 lymph node GTV_{Nx} volumes no similar 'outliers' could be identified with overall higher ADC values (see Fig. A.3).

4. Discussion

In this study we evaluated ΔADC in primary tumour and pathologic lymph nodes during radiotherapy treatment and found consistent increases at both sites. Furthermore ADC measurements can be acquired using T2-based delineations, as long as there is no shift between T2 and ADC mapping. This study has not conclusively identified an appropriate cut-off point for the ΔADC in GTV_{ADC} for identifying patients that would have an increased risk for recurrence, due to the low number of events in the study.

To our knowledge, this is the first study that investigates changes in whole pathologic lymph node ADC values during treatment. In

Table 2
Patients with recurrence (overall) after median follow-up of 15 months (range 7–22 months). Note that not all nodal recurrences could be found in retrospect on initial MRI before treatment. However, four of the 46 lymph nodes that were initially treated with a boost up to 55–60 Gy recurred. All regional recurrences included in-field nodal recurrences. In patient four, none of the lymph nodes that recurred were present at time of diagnose, therefore no ADC value could be derived during treatment.

Patient # with recurrence	1	2	3	4
FIGO stage	IIB	IIIB	IB2	IIA
Number of positive lymph nodes before treatment	10	4	0	2
Histopathologic subtype	SCC	SCC	AC	SCC
Time of recurrence after treatment (months)	6	9	12	12
Type of relapse (local/regional/distant)	regional/distant	regional/distant	local	regional
In field lymph nodes (yes/no)	yes	yes	n/a	yes
Number lymph nodes within/near high dose boost volume at time of recurrence	6	1	n/a	0
ΔADC in GTV_{ADC} or GTV_{Nx} between baseline and at 4 weeks during treatment (mm^2/s)	0.08; 0.57; 0.42	0.75	0.03	n/a*

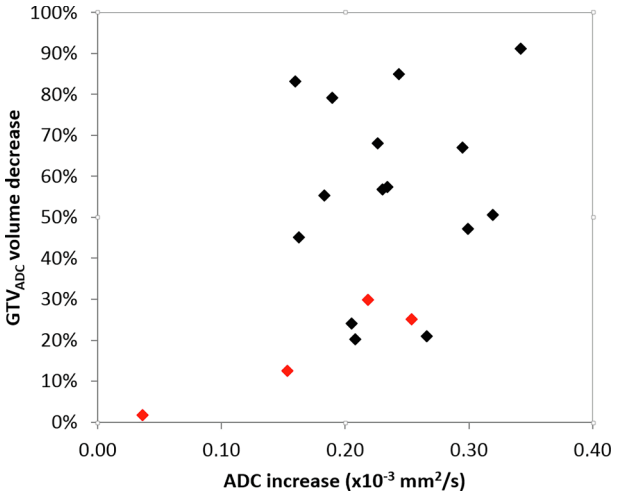

Fig. 5. Primary tumour volume (GTV_{ADC}) decrease in relation to ADC increase. There was no significant correlation found between the two parameters. Recurrences are visualised in red. (For interpretation of the references to colour in this figure legend, the reader is referred to the web version of this article.)

literature, pathologic lymph nodes have an ADC value of 0.77 and non-pathologic lymph nodes have an ADC value of 1.00–1.18 $\times 10^{-3}$ mm^2/s [24–26], with an optimal cut-off value of 0.86 $\times 10^{-3}$ mm^2/s based on mean ADC values in one single slice [26]. In our patients, baseline lymph node ADC values are below that threshold and rise to 1.13 $\times 10^{-3}$ mm^2/s during treatment, well above the suggested cut off value. Rising ADC values of primary tumour during treatment is confirmed by others [27,28]. Makino et al. found in 25 patients a rise from 0.89 to 1.25 $\times 10^{-3}$ mm^2/s respectively at baseline to 27–47 days after start of the treatment [28]. They found significantly larger ΔADC in the complete remission group (0.43 $\times 10^{-3}$ mm^2/s) compared to the residual tumour group (0.25 $\times 10^{-3}$ mm^2/s) [28]. A meta-analysis of Schreuder et al. found a similar ΔADC in complete responders (0.43 $\times 10^{-3}$ mm^2/s), and partial responders (0.26 $\times 10^{-3}$ mm^2/s) [23]. We only observed in one patient with a residual tumour a rise in the primary tumour ADC value of 0.03 $\times 10^{-3}$ mm^2/s which is consistent with their results.

Our study is limited by the relatively low number of patients and identified individual affected lymph nodes and the low number of events after treatment. Secondly, the follow-up period of 15 months is relatively short since 80% of the recurrences occur within up to 3 years after treatment [6,11,29]. However, this study corresponds well with former results in the literature; the primary tumour volume is reduced on average by 51% (literature 50%), and the lymph node tumour volume by 40% (literature 38%) [3,30,31]. Furthermore both ΔADC values of GTV and pathologic lymph nodes rise during treatment within the expected range. Another limitation was the small size of the lymph nodes making measurements of volume and ADC susceptible to greater uncertainty (see Fig. A.3). Furthermore, all 46 lymph nodes were analysed as being independently. However, within the same patient, tumour biology of within separate lymph nodes may be similar. During median follow-up of 15 months, lymph node relapse rate was 15% (literature 11–13%), and overall failure was 20% (literature 20%) [5,32–34].

Higher GTV ADC values were seen in four patients (Fig. A.3). Two of these cases show tumours that infiltrate around multiple benign cysts which have a high ADC value. Three of the four patients had adenocarcinomas and two of the four patients show regional recurrences. In future studies, ADC values in adenocarcinomas would be interesting to investigate, especially because of the well-known worse outcome of this histopathological type [35]. Additionally, it might be interesting to add a dynamic contrast enhanced (DCE) sequence to tumour assessment as some have found non-enhancement a potentially useful predictor for tumour recurrence [36].

Although there was no significant relation between ΔADC of tumour or lymph nodes and relapse, all four patients that relapsed (one local and three regional) showed little tumour reduction (median 19%, range 3–30%) in comparison with the group of non-relapsed patients (median 57%, range 21–100%) (Fig. 4). From past literature we have learned that initial tumour size (along with other clinical factors like FIGO stage and histopathologic subtype) and tumour response during EBRT are important prognostic factors for overall survival and LC [11,37]. Furthermore, available data indicate that FIGO > stage IB2 and (para-aortic) lymph node involvement before treatment is associated with higher chance of lymph node and distant relapse [5,13]. Recent literature from Schernberg et al., demonstrates significantly higher progression free survival and distant relapse free survival in patients that showed a GTV reduction > 90% during EBRT in a cohort of 255 patients treated with CRT and IGABT [38]. They also found significantly worse local, regional and distant outcomes when GTV and CTV_{HR} were > 7.5 cm^3 and > 25 cm^3 respectively at the time of brachytherapy. Therefore, the question is; could poor local response predict poor regional response to the same treatment that might ask for intensifying treatment? Schernberg et al. showed a relation between tumour reduction during EBRT and required dose to the $D_{90\%}$ of the CTV_{HR} for LC, however, they emphasised that more research is needed to identify those patients that would need dose escalation or dose de-escalation [38]. As IGABT has improved 5 year LC to > 90% for most patients [13], the EMBRACE II study [39] focuses on identifying risk factors for lymph node recurrences.

Primary tumour volume reduction during EBRT is, and ADC increase during EBRT might be, a good predictor for regional and distant control; however their relation is not fully clarified. Perhaps it is the tumour biology of the primary tumours and the lymph node metastasis and their response to treatment that link both outcomes. Therefore, other interventional strategies might be considered for patients with a higher risk of regional or distant recurrence, such as a higher dose to distant lesions which should always be applied with great caution.

In conclusion, as for primary tumours in the cervix, ADC values of affected nodes increase during EBRT. ADC values can be obtained from delineated volumes of primary tumour on T2 weighted MR unless there are substantial shifts between ADC mapping and T2 signal. Evaluation of ΔADC for primary tumours and affected lymph nodes might help to better predict response to EBRT and disease outcome. This study is in line with available evidence that volume reduction of the primary cervical tumour during EBRT is a prognostic factor for relapse.

Conflicts of interest

Cornelis van den Berg is a minority share holder of MRCode BV. The other authors declare that there are no conflicts of interest.

Role of funding source

The authors declare that no study sponsors were involved.

Acknowledgements

We kindly acknowledge Simon Woodings, medical physicist at the Department of Radiation Oncology of the University Medical Centre Utrecht, for his thorough revisions and support.

Appendix A. Supplementary data

Supplementary data to this article can be found online at https://doi.org/10.1016/j.phro.2019.03.001.

References

[1] Ferlay J, Soerjomataram I, Ervik M, Dikshit R, Eser S, Mathers C, et al. Cancer Today / GLOBOCAN 2012 v1.0: Estimated Cancer Incidence, Mortality and Prevalence Worldwide in 2012: IARC CancerBase No. 11, WHO-World Heal Organ / IARC. Int Agency Res Cancer 2014. http://globocan.iarc.fr (accessed November 12, 2017).

[2] Lim K, Small W, Portelance L, Creutzberg C, Jürgenliemk-Schulz IM, Mundt A, et al. Consensus guidelines for delineation of clinical target volume for intensity-modulated pelvic radiotherapy for the definitive treatment of cervix cancer. Int J Radiat Oncol Biol Phys 2011;79:348–55. https://doi.org/10.1016/j.ijrobp.2009.10.075.

[3] van de Bunt L, van der Heide UA, Ketelaars M, de Kort GAP, Jürgenliemk-Schulz IM. Conventional, conformal, and intensity-modulated radiation therapy treatment planning of external beam radiotherapy for cervical cancer: The impact of tumor regression. Int J Radiat Oncol Biol Phys 2006;64:189–96. https://doi.org/10.1016/j.ijrobp.2005.04.025.

[4] de Boer P, Jürgenliemk-Schulz IM, Westerveld H, de Leeuw AAC, Dávila-Fajardo R, Rasch CRN, et al. Patterns of care survey: Radiotherapy for women with locally advanced cervical cancer. Radiother Oncol 2017;123:306–11. https://doi.org/10.1016/j.radonc.2017.04.005.

[5] Sturdza A, Pötter R, Fokdal LU, Haie-Meder C, Tan LT, Mazeron R, et al. Image guided brachytherapy in locally advanced cervical cancer: Improved pelvic control and survival in RetroEMBRACE, a multicenter cohort study. Radiother Oncol 2016;120:428–33. https://doi.org/10.1016/j.radonc.2016.03.011.

[6] Nomden CN, De Leeuw AAC, Roesink JM, Tersteeg RJHA, Moerland MA, Witteveen PO, et al. Clinical outcome and dosimetric parameters of chemo-radiation including MRI guided adaptive brachytherapy with tandem-ovoid applicators for cervical cancer patients: A single institution experience. Radiother Oncol 2013;107:69–74. https://doi.org/10.1016/j.radonc.2013.04.006.

[7] Kusmirek J, Robbins J, Allen H, Barroilhet L, Anderson B, Sadowski EA. PET/CT and MRI in the imaging assessment of cervical cancer. Abdom Imaging 2015;40:2486–511. https://doi.org/10.1007/s00261-015-0363-6.

[8] Kang S, Kim S, Chung D, Seo S, Kim J, Nam B, et al. Diagnostic value of 18F-FDG PET for evaluation of paraaortic nodal metastasis in patients with cervical carcinoma: a meta-analysis. J Nucl Med 2016;51:360–7. https://doi.org/10.2967/jnumed.109.066217.

[9] Pötter R, Haie-Meder C, Van Limbergen E, Barillot I, De Brabandere M, Dimopoulos J, et al. Recommendations from gynaecological (GYN) GEC ESTRO working group (II): concepts and terms in 3D image-based treatment planning in cervix cancer brachytherapy-3D dose volume parameters and aspects of 3D image-based anatomy, radiation physics, radiobiology. Radiother Oncol 2006;78:67–77. https://doi.org/10.1016/j.radonc.2005.11.014.

[10] Haie-Meder C, Pötter R, Van Limbergen E, Briot E, De Brabandere M, Dimopoulos J, et al. Recommendations from Gynaecological (GYN) GEC-ESTRO Working Group (I): concepts and terms in 3D image based 3D treatment planning in cervix cancer brachytherapy with emphasis on MRI assessment of GTV and CTV. Radiother Oncol 2005;74:235–45. https://doi.org/10.1016/j.radonc.2004.12.015.

[11] Tanderup K, Fokdal LU, Sturdza A, Haie-Meder C, Mazeron R, van Limbergen E, et al. Effect of tumor dose, volume and overall treatment time on local control after radiochemotherapy including MRI guided brachytherapy of locally advanced cervical cancer. Radiother Oncol 2016;120:441–6. https://doi.org/10.1016/j.radonc.2016.05.014.

[12] Pötter R, Georg P, Dimopoulos JC, Grimm M, Berger D, Nesvacil N, et al. Clinical outcome of protocol based image (MRI) guided adaptive brachytherapy combined with 3D conformal radiotherapy with or without chemotherapy in patients with locally advanced cervical cancer. Radiother Oncol 2011;100:116–23. https://doi.org/10.1016/j.radonc.2011.07.012.

[13] Pötter R, Tanderup K, Kirisits C, de Leeuw A, Kirchheiner K, Nout R, et al. The EMBRACE II study: The outcome and prospect of two decades of evolution within the GEC-ESTRO GYN working group and the EMBRACE studies. Clin Transl Radiat Oncol 2018;9:48–60. https://doi.org/10.1016/j.ctro.2018.01.001.

[14] Engin G. Cervical cancer: MR imaging findings before, during, and after radiation therapy. Eur Radiol 2006;16:313–24. https://doi.org/10.1007/s00330-005-2804-z.

[15] de Boer P, Bleeker MCG, Spijkerboer AM, van de Schoot AJ, Bipat S, Buist MR, et al. Craniocaudal tumour extension in uterine cervical cancer on MRI compared to histopathology. Eur J Radiol Open 2015;2:111–7. https://doi.org/10.1016/j.ejro.2015.07.001.

[16] Padhani AR, Liu G, Mu-Koh D, Chenevert TL, Thoeny HC, Takahara T, et al. Diffusion-weighted magnetic resonance imaging as a cancer biomarker: consensus and recommendations. Neoplasia 2009;11:102–25. https://doi.org/10.1593/neo.81328.

[17] Whittaker CS, Coady A, Culver L, Rustin G, Padwick M, Padhani AR. Diffusion-weighted MR imaging of female pelvic tumors: a pictorial review. Radiographics 2009;29:759–74. https://doi.org/10.1148/rg.293085130. discussion 774–8.

[18] Chen YB, Hu CM, Chen GL, Hu D, Liao J. Staging of uterine cervical carcinoma: whole-body diffusion-weighted magnetic resonance imaging. Abdom Imaging 2011;36:619–26. https://doi.org/10.1007/s00261-010-9642-4.

[19] Rizzo S, Summers P, Raimondi S, Belmonte M, Maniglio M, Landoni F, et al. Imaging pesato in diffusione per la valutazione della risposta a terapie non chirurgiche del tumore della cervice uterina. Radiol Medica 2011;116:766–80. https://doi.org/10.1007/s11547-011-0650-4.

[20] Liu Y, Bai R, Sun H, Liu H, Zhao X, Li Y. Diffusion-weighted imaging in predicting and monitoring the response of uterine cervical cancer to combined chemoradiation. Clin Radiol 2009;64:1067–74. https://doi.org/10.1016/j.crad.2009.07.010.

[21] Onal C, Erbay G, Guler OC. Treatment response evaluation using the mean apparent diffusion coefficient in cervical cancer patients treated with definitive chemoradiotherapy. J Magn Reson Imaging 2016;44:1010–9. https://doi.org/10.1002/jmri.25215.

[22] Liu Y, Sun H, Bai R, Ye Z. Time-window of early detection of response to concurrent chemoradiation in cervical cancer by using diffusion-weighted MR imaging: A pilot study. Radiat Oncol 2015;10:1–8. https://doi.org/10.1186/s13014-015-0493-6.

[23] Schreuder SM, Lensing R, Stoker J, Bipat S. Monitoring treatment response in patients undergoing chemoradiotherapy for locally advanced uterine cervical cancer by additional diffusion-weighted imaging: A systematic review. J Magn Reson Imaging 2015;42:572–94. https://doi.org/10.1002/jmri.24784.

[24] Kwee TC, Takahara T, Luijten PR, Nievelstein RAJ. ADC measurements of lymph nodes: Inter- and intra-observer reproducibility study and an overview of the literature. Eur J Radiol 2010;75:215–20. https://doi.org/10.1016/j.ejrad.2009.03.026.

[25] Lin G, Ho KC, Wang JJ, Ng KK, Wai YY, Chen YT, et al. Detection of lymph node metastasis in cervical and uterine cancers by diffusion-weighted magnetic resonance imaging at 3T. J Magn Reson Imaging 2008;28:128–35. https://doi.org/10.1002/jmri.21412.

[26] Jeong KK, Kyoung AK, Park BW, Kim N, Cho KS. Feasibility of diffusion-weighted imaging in the differentiation of metastatic from nonmetastatic lymph nodes: Early experience. J Magn Reson Imaging 2008;28:714–9. https://doi.org/10.1002/jmri.21480.

[27] Meng J, Zhu L, Zhu L, Xie L, Wang H, Liu S, et al. Whole-lesion ADC histogram and texture analysis in predicting recurrence of cervical cancer treated with CCRT. Oncotarget 2017;8:92442–53. https://doi.org/10.18632/oncotarget.21374.

[28] Makino H, Kato H, Furui T, Morishige K, Kanematsu M. Predictive value of diffusion-weighted magnetic resonance imaging during chemoradiotherapy for uterine cervical cancer. J Obstet Gynaecol Res 2014;40:1098–104. https://doi.org/10.1111/jog.12276.

[29] Elit L, Fyles AW, Devries MC, Oliver TK, Fung-Kee-Fung M. Follow-up for women after treatment for cervical cancer: A systematic review. Gynecol Oncol 2009;114:528–35. https://doi.org/10.1016/j.ygyno.2009.06.001.

[30] Beadle BM, Jhingran A, Salehpour M, Sam M, Iyer RB, Eifel PJ. Cervix regression and motion during the course of external beam chemoradiation for cervical cancer. Int J Radiat Oncol Biol Phys 2009;73:235–41. https://doi.org/10.1016/j.ijrobp.2008.03.064.

[31] Yoon MS, Nam T-K, Chung W-K, Jeong SY, Ahn S-J, Nah B-S, et al. Metabolic response of pelvic and para-aortic lymph nodes during radiotherapy for carcinoma of the uterine cervix: using positron emission tomography/computed tomography. Int J Gynecol Cancer 2011;21:699–705. https://doi.org/10.1111/IGC.0b013e3181e94349.

[32] Tan LT, Kirchheiner K, Sturdza A, Fokdal L, Haie-Meder C, Jurgenliemk-Schulz IM, et al. Impact of image-guided brachytherapy on pattern of relapse in the RetroEMBRACE cervix cancer study. Radiother Oncol 2018;127:S201. https://doi.org/10.1016/S0167-8140(18)30702-3.

[33] Nomden CN, Pötter R, de Leeuw AAC, Tanderup K, Lindegaard JC, Schmid MP, et al. Nodal failure after chemo-radiation and MRI guided brachytherapy in cervical cancer: Patterns of failure in the EMBRACE study cohort. Radiat Oncol 2019;134:185–90. https://doi.org/10.1016/j.radonc.2019.02.007.

[34] Taylor A, Rockall AG, Powell MEB. An atlas of the pelvic lymph node regions to aid radiotherapy target volume definition. Clin Oncol (R Coll Radiol) 2007;19:542–50. https://doi.org/10.1016/j.clon.2007.05.002.

[35] Farley JH, Hickey KW, Carlson JW, Rose GS, Kost ER, Harrison TA. Adenosquamous histology predicts a poor outcome for patients with advanced-stage, but not early-stage, cervical carcinoma. Cancer 2003;97:2196–202. https://doi.org/10.1002/cncr.11371.

[36] Mannelli L, Patterson AJ, Zahra M, Priest AN, Graves MJ, Lomas DJ, et al. Evaluation of nonenhancing tumor fraction assessed by dynamic contrast-enhanced MRI subtraction as a predictor of decrease in tumor volume in response to chemoradiotherapy in advanced cervical cancer. Am J Roentgenol 2010;195:524–7. https://doi.org/10.2214/AJR.09.3437.

[37] Wang JZ, Mayr NA, Zhang D, Li K, Grecula JC, Montebello JF, et al. Sequential magnetic resonance imaging of cervical cancer. Cancer 2010;116:5093–101. https://doi.org/10.1002/cncr.25260.

[38] Schernberg A, Bockel S, Annede P, Fumagalli I, Escande A, Mignot F, et al. Tumor shrinkage during chemoradiation in locally advanced cervical cancer patients: prognostic significance, and impact for image-guided adaptive brachytherapy. Int J Radiat Oncol Biol Phys 2018;102:362–72. https://doi.org/10.1016/j.ijrobp.2018.06.014.

[39] EMBRACE II https://www.embracestudy.dk. (Accessed 10 July 2018).